第 43 卷 第 10 期/2023 年 5 月/光学学报 研究论文

光学学报

多级衍射元件消色差系统的面型分析

郑博洋[1,2]，薛常喜[1,2*]

[1]长春理工大学光电工程学院，吉林 长春 130022；

[2]长春理工大学先进光学设计与制造技术吉林省高校重点实验室，吉林 长春 130022

摘要 多级衍射元件在衍射望远系统消色差领域的应用逐渐成为热点。基于赛德尔三级像差理论，对由多级衍射光学元件、折射光学元件和菲涅耳衍射元件三元件组合的光学系统展开分析。在400～700 nm工作波段，通过数学推导校正表面系统的球差，同时实现消色差及复消色差。对系统在平面、球面和非球面不同面型下的成像质量进行比对。当系统为非球面设计时，调制传递函数在截止频率50 lp/mm处高于0.6683，优于平面和球面设计，衍射圈入能量更高，成像质量更好。该研究为将多级衍射元件组合系统运用到消色差领域提供了参考。

关键词 衍射；多级衍射元件；三级像差理论；消色差；非球面；折衍射混合

中图分类号 O436 **文献标志码** A **DOI**：10.3788/AOS221950

1 引 言

随着光学技术的日益发展与创新，光学系统的性能与指标愈发具有挑战性，光学系统始终往便于加工、轻量化、制造成本低等方向发展。其中，多级衍射元件（MOD）的质量轻、基于多级衍射元件的光学系统体积小且结构不复杂，能够改善系统成像质量，提供大视场[1-4]，元件便于折叠和展开，可用于空间望远镜[5]、太赫兹成像[6]、光束整形[7]、遥感[8]等领域的轻量级光学元件中。可以发现，单片多级衍射透镜可通过分区方式实现宽波段的成像需求[9]，但衍射效率较低，其自身的色散特性限制了透镜在宽波段中的应用。国内外较多单位开展了关于衍射元件消色差的研究[10-11]，利用组合衍射元件来实现系统消色差，大大增加了宽波段条件下衍射镜头的实用性。在宽波段领域，利用组合衍射元件可实现高衍射效率的折衍射混合光学系统，使光学系统的成像质量得到提高[12-13]。Sweeney等[14-15]提出通过将简单衍射透镜（级次M=1）叠加到多级衍射透镜上来修正材料带来的色差的方法，也使用了低M数多衍射元件透镜对透镜背面进行色差校正。文献[16]描述了多级衍射工程（MODE）透镜的原理，系统前表面是一个高M数多级衍射透镜，系统背面为菲涅耳透镜，该文献分析了衍射元件与折衍射混合元件组合消色差的性能，并给出了具体的元件设计。通过对成型元件进行有效的复制，将多级衍射元件的组合系统运用到鹦鹉螺天文台的观测中[5,17]，这为系外行星的研究提供了大孔径空间望远镜阵列。多级衍射元件组合光学系统的设计研究中没有对系统的面型特征进行比较的内容。针对组合系统消色差及成像方面的工作，首先对多级衍射元件组合系统的三级像差进行计算，接着利用Zemax软件对系统的面型展开对比和分析，并选出最优结果。

2 基本原理

2.1 标量衍射理论

衍射光学的理论模型可分为标量衍射理论模型和矢量衍射理论模型。其中，标量衍射理论可应用于输出平面较衍射元件距离足够远和入射光波长远小于微结构周期宽度的衍射光学元件的设计与分析中，其通常将衍射元件作为一种薄透镜模型（光学元件为无限薄的曲面），此时可用复振幅透过率函数来表示衍射光学元件对入射光场的调制作用。成像衍射光学元件的设计基础通常是使用标量衍射理论模型，本文基于光波的标量衍射理论，对多级衍射光学元件组合系统的成像特性展开对比研究。

2.2 多级衍射元件组合系统的三级像差表示

Sweatt等[18-20]将平面基底的全息透镜（衍射元件）等效为普通薄透镜，给出了菲涅耳透镜薄透镜模型下的三级像差公式。由此可见，衍射光学元件从数学角度来说等同于薄透镜，其折射率无限，可以使用几何光学的相关理论分析成像特性，运用三级像差公式来对系统进行分析研究[21-22]。因此，对于多级衍射元件与

收稿日期：2022-11-07；**修回日期**：2022-12-12；**录用日期**：2022-12-19；**网络首发日期**：2023-01-06

基金项目：吉林省自然科学基金（20220101124JC）

通信作者：*xcx272479@sina.com

折衍射混合元件的消色差系统设计，本文基于薄透镜模型展开计算。选择的多级衍射元件组合系统为多级衍射元件、折射光学元件（ROE）和菲涅耳衍射元件（DFL）三元件胶合的系统模型，具体系统示意图如图1（a）所示，前后表面示意图如图1（b）和图1（c）所示。本节通过对系统弯曲参量、共轭参量和透镜曲率的表达和计算，同时校正三个元件胶合的折衍射混合复消色差光学系统的球差和彗差。

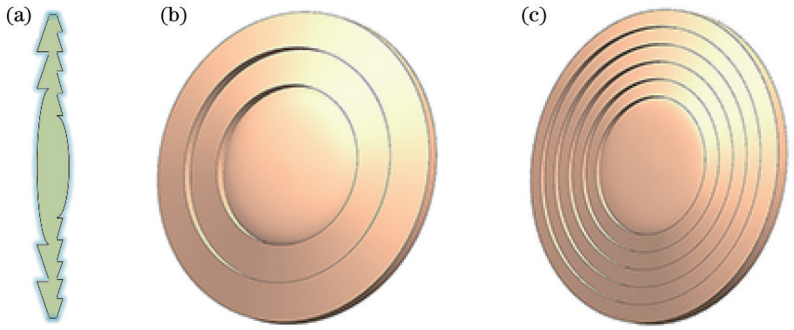

图1　多级衍射元件组合系统示意图。(a)具体系统图；(b)系统正面图；(c)系统后表面图

Fig. 1　Schematic diagrams of combined system of multiple-order diffraction elements. (a) Specific system diagram; (b) system front surface diagram; (c) system rear surface diagram

假设系统的总光焦度为K，MOD、ROE、DFL三个元件的光焦度为K_1、K_2、K_3，阿贝数为v_1、v_2、v_3，相对部分色散为P_1、P_2、P_3，根据其消色差和复消色差特性，可以得出

$$\begin{cases} K_1+K_2+K_3=K \\ \dfrac{K_1}{v_1}+\dfrac{K_2}{v_2}+\dfrac{K_3}{v_3}=0 \\ \dfrac{K_1}{v_1}P_1+\dfrac{K_2}{v_2}P_2+\dfrac{K_3}{v_3}P_3=0 \end{cases}, \tag{1}$$

$$\begin{cases} M=v_2(P_3-P_1)+v_1(P_2-P_3)+v_3(P_1-P_2) \\ K_1=\dfrac{Kv_1(P_2-P_3)}{M} \\ K_2=\dfrac{Kv_2(P_3-P_1)}{M} \\ K_3=\dfrac{Kv_3(P_1-P_2)}{M} \end{cases}。 \tag{2}$$

因为三个光学元件是胶合的（密接结构），所以第一近轴光线与透镜的交高近似相等，即$y_1=y_2=y_3=y$，忽略衍射元件的高次项，根据薄透镜的三级像差理论得到三元件胶合后的三级像差系数为

$$S_{\mathrm{I}}=\frac{y^4}{4}\left\{K_1^3\left(1+B_1^2+4B_1C_1+3C_1^2\right)+K_2^3\left[\left(\frac{n_2}{n_2-1}\right)^2+\frac{n_2+2}{n_2(n_2-1)^2}B_2^2+\frac{4(n_2+1)}{n_2(n_2-1)}B_2C_2+\frac{3n_2+2}{n_2}C_2^2\right]+K_3^3\left[1+B_3^2+4B_3C_3+3C_3^2\right]\right\}, \tag{3}$$

$$S_{\mathrm{II}}=-\frac{y^2H}{2}\left\{K_1^2(B_1+2C_1)+K_2^2\left[\frac{n_2+1}{n_2(n_2-1)}B_2+\frac{2n_2+1}{n_2}C_2\right]+K_3^2(B_3+2C_3)\right\}, \tag{4}$$

$$S_{\mathrm{III}}=H^2(K_1+K_2+K_3), \tag{5}$$

$$S_{\mathrm{IV}}=H^2\frac{K_2}{n_2}, \tag{6}$$

$$S_{\mathrm{V}}=0, \tag{7}$$

式中：S_{I}、S_{II}、S_{III}、S_{IV}和S_{V}分别代表系统的球差、彗差、像散、场曲和畸变的赛德尔像差系数；B_1、B_2和B_3为三个元件的弯曲参量。

当平行光入射（即入射角为0°）时，由薄透镜的共轭角定义和关系表达式可得

$$C_1=-1, \tag{8}$$

$$\frac{K_1}{2}(C_1-1)=\frac{K_2}{2}(C_2+1), \tag{9}$$

$$\frac{K_2}{2}(C_2-1)=\frac{K_3}{2}(C_3+1), \tag{10}$$

式中：C_1、C_2和C_3分别为第1个、第2个、第3个元件的共轭参量。

$$B_1=\frac{2c_{s1}}{K_1}, \tag{11}$$

$$B_2=\frac{2c_{s3}}{K_3}, \tag{12}$$

$$c_{s1}=c_{21}=\frac{B_1K_1}{2}=\frac{K_2}{2(n_2-1)}(B_2+1),\quad(13)$$

$$c_{s3}=c_{22}=\frac{B_3K_3}{2}=\frac{K_2}{2(n_2-1)}(B_2-1),\quad(14)$$

式中：c_{s1}、c_{s3}分别表示第1个、第3个DOE的基底曲率；c_{21}、c_{22}分别表示第2个ROE的前后表面曲率，因为前后表面双胶合，所以胶合面曲率相等。

进一步化简可得

$$B_1=\frac{K_2(B_2+1)}{K_1(n_2-1)},\quad(15)$$

$$B_3=\frac{K_2(B_2-1)}{K_3(n_2-1)},\quad(16)$$

$$B_2=\frac{B_1K_1(n_2-1)}{K_2}-1=\frac{B_3K_3(n_2-1)}{K_2}-1。\quad(17)$$

令$S_{\mathrm{I}}=0$，校正球差，得出一个关于B_2的一元二次方程，即

$$\alpha B_2^2+\beta B_2+\gamma=0,\quad(18)$$

$$\alpha=\frac{K_1K_2^2n_2+K_2^3(n_2+2)+K_3K_2^2n_2}{n_2(n_2-1)^2},\quad(19)$$

$$\beta=\frac{2K_2^2(K_1-K_3)}{(n_2-1)^2}+\frac{4K_2(K_1^2C_1+K_3^2C_3)}{n_2-1}+\frac{K_2^3 4(n_2+1)C_2}{n_2(n_2-1)},\quad(20)$$

$$\gamma=\frac{K_2^2(K_1+K_3+K_2n_2^2)}{(n_2-1)^2}+\frac{4K_2(K_1^2C_1-K_3^2C_3)}{n_2-1}-\frac{K_2^3C_2^2(3n_2+2)}{n_2}+K_1^3(1+3C_1^2)+K_3^3(1+3C_3^2)。\quad(21)$$

根据以上的赛德尔像差理论和折衍射混合复消色差原理[式(2)]，本文设计的多级衍射元件组合的光学系统可消除系统球差、彗差并复消色差。在系统面型分析与设计时，主要考虑以下几个比较参数：对于扩大光谱范围，传统意义上，通常要考虑消色差因素和材料因素，即在宽光谱范围内对材料进行加工处理；在视场对光学系统的影响下，系统畸变通常会增加，导致衍射效率降低，从而导致系统成像质量降低；光学系统设计中另一个重要的参数是孔径值，这个参数不仅决定了系统衍射有限的空间分辨率，更重要的是决定了系统能收集的光量，但随着入瞳直径的增加，孔径较大的光学表面的制造，尤其是对非球面的加工仍充满挑战。为了便于计算和分析，令该系统焦距f为20 mm，入瞳直径为5 mm，系统工作波段为400～700 nm的可见光波段，要求复消色差波长光为F光(486.1327 nm)、d光(587.5618 nm)和C光(656.2725 nm)，中心波长为d光。

采用聚甲基丙烯酸甲酯(PMMA)和聚碳酸酯(PC)分别作为多级衍射元件和菲涅耳元件的基底材料，聚苯乙烯(PS)作为折射元件基底材料，实现系统复消色差、校正球差后，由式(18)～(21)得出有关B_2的一元二次函数图，如图2所示。

令该系统中$S_{\mathrm{II}}=0$，校正彗差，简化得到一个B_2的关系表达式，即

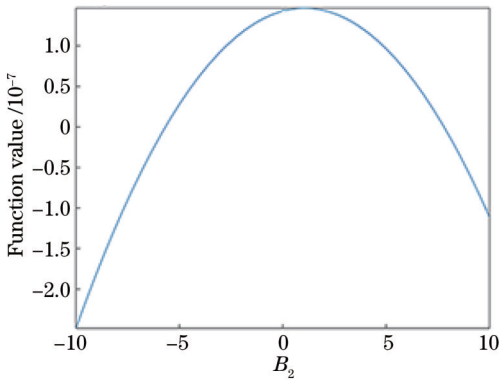

图2　球差为0时衍射元件弯曲参量B_2的函数图

Fig. 2　Function of bending parameter B_2 of diffraction element when spherical aberration is 0

$$B_2=\frac{(2n_2-2n_2^2)(K_1^2C_1+K_3^2C_3)-(2n_2^2-n_2-1)K_2^2C_2+K_2n_2(K_3-K_1)}{K_2(K_1n_2+K_3n_2+n_2+1)},\quad(22)$$

代入数据可得，此时系统B_2=−0.0012。由式(13)、(14)可得出曲率$c_{s1}=-1.082\times10^{-3}$，$c_{s3}=1.085\times10^{-3}$。把上述数据输入光学设计软件Zemax，得到的模拟结果如图3所示，结果表明系统校正了球差和彗差，同时实现了复消色差，其中横坐标p_x、p_y为x、y方向上的归一化光瞳坐标，纵坐标e_x、e_y为在像平面x、y方向上的位置坐标。

3　面型分析与讨论

与现有技术相比，本文设计系统的有益效果为：采用三元件组合系统结构、利用折衍射混合系统平衡像差并利用菲涅耳元件的衍射特性实现宽波段成像、系统成像质量得到改善、系统体积和质量减小。

通常情况下，不同面型的设计对折衍射混合消色差系统至关重要。相较于传统的平面面型，应用球面、

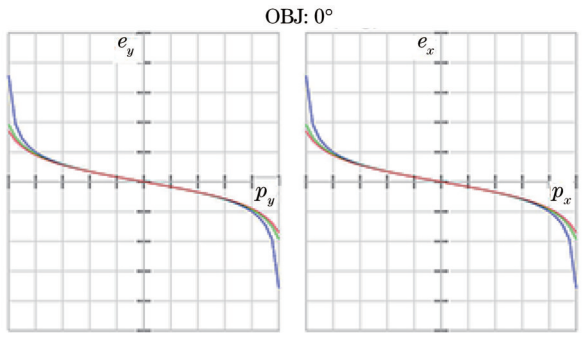

图 3　多级衍射元件组合系统的像差曲线

Fig. 3　Aberration curves of combined system with multiple-order diffractive elements

非球面或自由曲面的成像光学系统具有更高的设计自由度，且像差校正能力较强，在系统中也承担更多的平衡像差的任务，更易实现系统小型化、轻量化的设计目标。本节对三光学元件的胶合形式进行分析，对其不同表面形貌进行对比，选择出更优的表面。接下来主要从平面、球面、非球面三种模式下对比三个元件的消色差和成像质量情况。

分别将系统置于平面、球面、非球面基底下，具体光学结构如图 4 所示。利用 Zemax 软件对不同面型下的系统成像质量进行对比分析。表 1 为系统在平面、球面和非球面基底下的光学系统参数，三种面型下选用相同的材料且材料厚度相同。

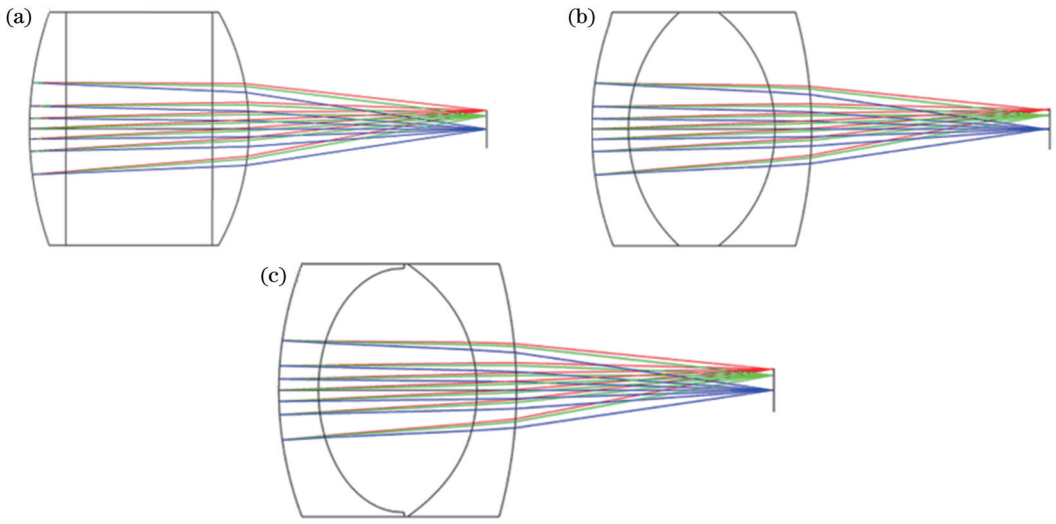

图 4　三元件双胶合系统的光学结构图。(a)平面面型；(b)球面面型；(c)非球面面型

Fig. 4　Optical structure diagrams of three-element double gluing system. (a) Planar surface type; (b) spherical surface type; (c) aspheric surface type

表 1　系统在平面、球面及非球面基底下的光学系统参数

Table 1　Optical system parameters of the system under planar, spherical, and aspheric surface substrates

Surface	Type	Radius /mm			Thickness / mm	Glass material	2^{nd} order term (aspheric)	4^{th} order term (aspheric)
		Plane	Spherical	Aspheric				
Object	Standard		Infinity		Infinity	—	—	—
1	Standard	19.117	17.809	17.809	2	N-SF15	—	—
2	Binary 2	Infinity	8.673	8.673	8	N-SSK2	−0.0057	-4.159×10^{-5}
3	Binary 2	Infinity	−8.085	−8.085	2	LLF1	0.2905	-6.201×10^{-4}
Stop	Standard	Infinity	−23.497	−23.497	13	—	—	—
Image	Standard		Infinity		—	—	—	—

不同系统下的弧度系数如表 2 所示，其中 p 表示平面，s 表示球面，a 表示非球面，p 为系统的径向坐标，p_2 的系数为二次位相系数，决定衍射元件的傍轴光焦度，p_4 和 p_6 的系数为非球面位相系数，多用于校正系统的单色像差。选择系统焦距 f=20 mm，视场为 3.5°，F 数为 4，工作波段为 400～700 nm 可见光波段。

图 5(a)～(c)分别显示了平面、球面和非球面类型下的系统成像质量，图 6(a)～(c)显示了相应表面类型下的轴向像差图。与平面成像质量相比，当系统为球面和非球面表面面型时，光学系统的成像质量更好，消色差效果更明显。

图 6 横坐标为光轴方向的位置坐标(单位为 mm)，纵坐标为归一化光瞳坐标，可以从中看出球面和非球面面型下的消色差效果较好，接着比较了这两个面型下的其他度量标准。一个度量是调制传递函数(MTF)，这是评价光学系统性能的重要参数，是衡量

表 2 系统在平面、球面及非球面面型下的弧度系数

Table 2 Arc coefficients of the system for planar, spherical, and aspheric surfaces

Type	Coefficient on p^2			Coefficient on p^4			Coefficient on p^6		
	p	s	a	p	s	a	p	s	a
Binary 2	-9.7×10^4	-8.5×10^4	-3.1×10^4	1.3×10^8	3.2×10^8	1.6×10^8	-4.2×10^{10}	-2.9×10^{11}	-1.1×10^{11}
Binary 2	-1.5×10^5	-8.9×10^4	-1.2×10^5		—			—	

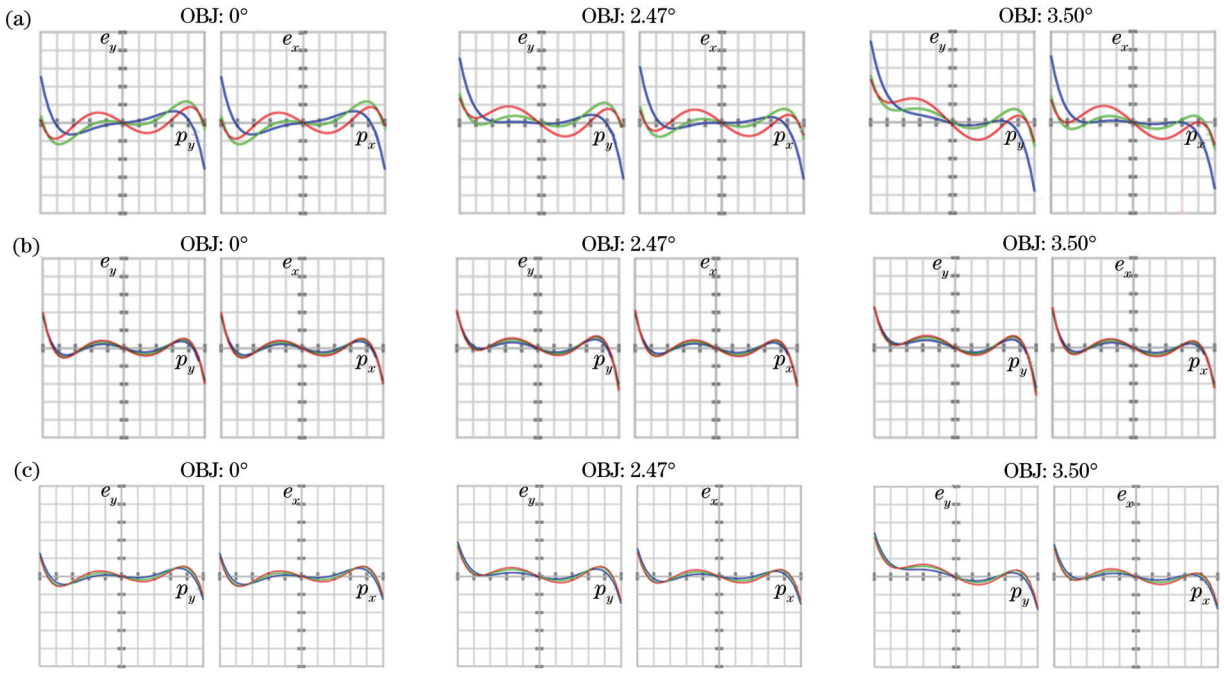

图 5 平面、球面、非球面面型下对应的系统成像质量。(a)平面;(b)球面;(c)非球面

Fig. 5 System imaging quality of systems with planar, spherical, and aspheric surface types. (a) Planar surface; (b) spherical surface; (c) aspheric surface

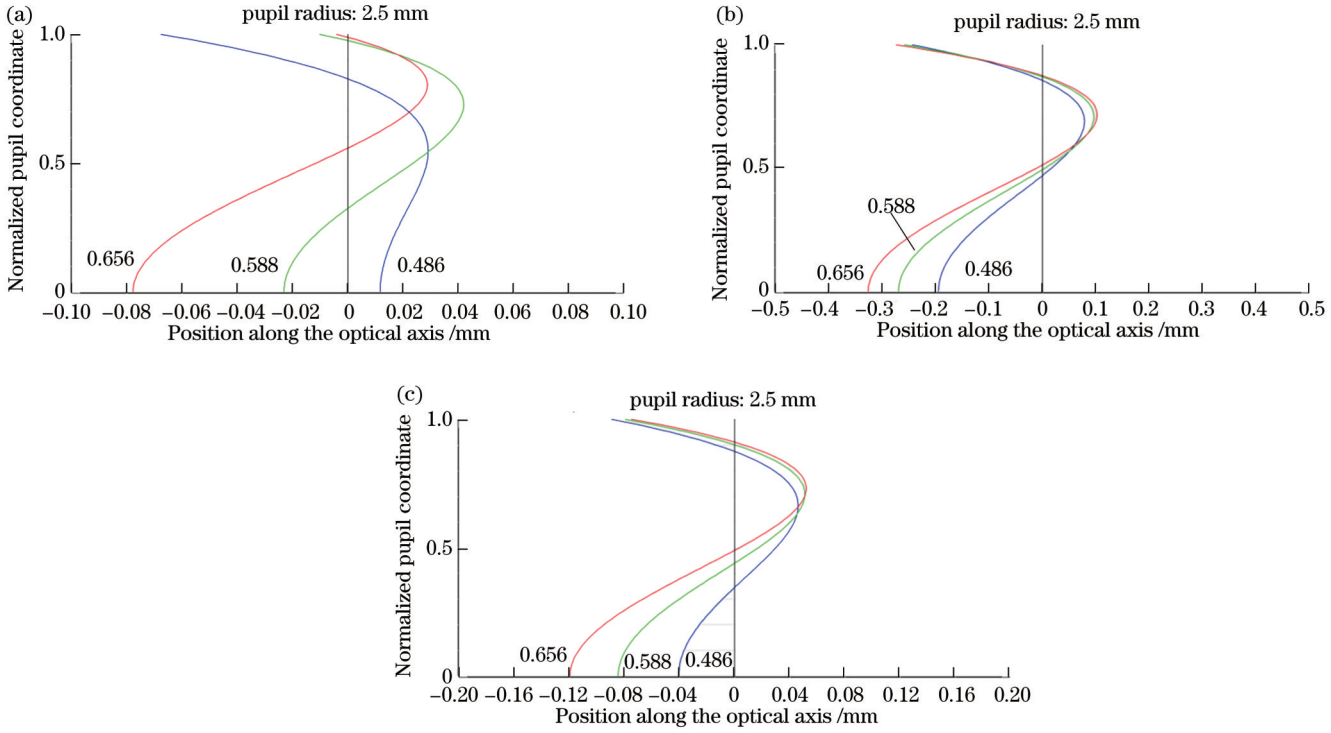

图 6 三种表面类型的轴向像差。(a)平面;(b)球面;(c)非球面

Fig. 6 Axial aberration of three surface types. (a) Planar surface; (b) spherical surface; (c) aspheric surface

系统图像质量的重要参数之一。另一个度量是圈入能量(EE),它是在一个特定直径内的能量除以总聚焦功率的百分比,在越小光斑半径内圈入能量越高,则表明光斑聚焦效果越好。

球面和非球面面型下的MTF值如图7所示。从图7(a)可以看出,当系统为球面面型时,在50 lp/mm的截止频率处,MTF值高于0.3653。从图7(b)可以看出,当系统为非球面面型时,MTF值在截止频率处高于0.6683。因此,在相同截止频率处,非球面面型下系统的成像质量更好。从图7(c)、(d)不难看出,非球面面型下衍射圈入能量更高。

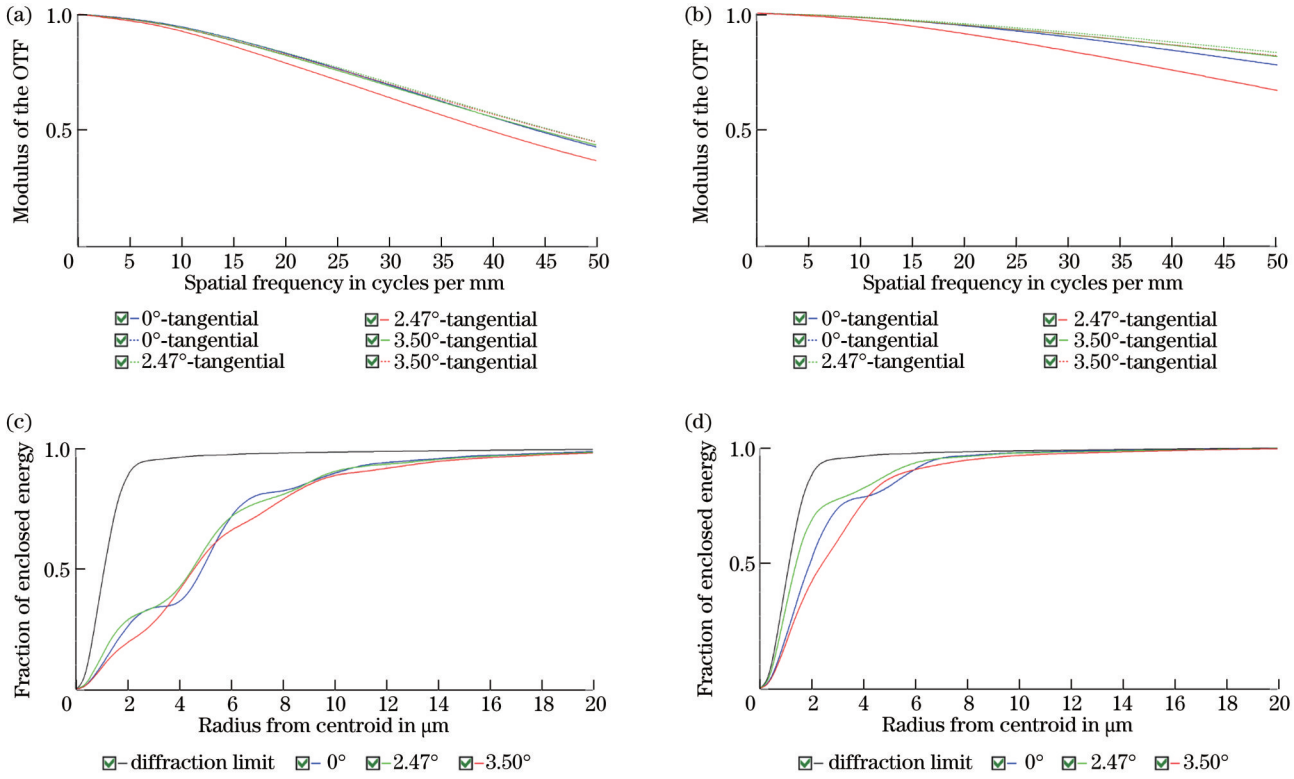

图7　球面和非球面面型下系统的成像质量图。(a)球面面型下的MTF;(b)非球面面型下的MTF;(c)球面面型下的衍射圈入能量;(d)非球面面型下的衍射圈入能量

Fig. 7　Imaging quality of the system under spherical and aspheric surfaces. (a) MTF for spherical surface; (b) MTF for aspheric surface; (c) diffraction encircled energy for spherical surface; (d) diffraction encircled energy for aspheric surface

综上所述,当多级衍射元件、折射元件和菲涅耳元件三元件胶合时,相较于平面面型,系统为球面、非球面面型时的成像质量更好,消色差效果更明显。但在非球面面型情况下,在截止频率50 lp/mm处,系统的MTF值远高于系统在球面面型下的MTF值,且衍射圈入能量更高。因此,三元件组合系统在非球面面型时更满足消色差要求且成像质量更好。非球面光学与球面光学相比有很大的优势,非球面可以提高系统的相对口径比,扩大视场角,在提高光束质量的同时透镜数比球面构成的系统少,且镜头的小型化可减小系统质量。

4　结　　论

基于标量衍射理论,提出了消色差多级衍射元件的设计,该设计对多级衍射元件应用于宽波段的消色差光学系统设计具有指导意义。对由多级衍射元件、折射元件和菲涅耳衍射元件三元件组合的系统展开分析,基于赛德尔像差理论,给定工作波段为400~700 nm,运用三级像差公式,通过对系统弯曲参量、共轭参量和透镜曲率的表达和计算,实现三个元件胶合的折衍射混合复消色差系统的球差和彗差的同时校正。对该系统的面型情况进行分析,对其在平面、球面和非球面情况下的消色差情况、系统成像质量展开比较,发现系统在非球面面型时的成像质量更好,衍射圈入能量更多,消色差效果更明显。该系统的体积小、质量轻且结构简单,在空间光学领域的应用前景广阔。

参　考　文　献

[1] Brown D M, Kathman A D. Off-axis spherical element telescope with binary optic corrector[J]. Proceedings of SPIE, 1991, 1555: 114-127.

[2] Stone T, George N. Hybrid diffractive-refractive lenses and achromats[J]. Applied Optics, 1988, 27(14): 2960-2971.

[3] Swanson G J, Veldkamp W B. Diffractive optical elements for use in infrared systems[J]. Optical Engineering, 1989, 28(6): 605-608.

[4] Sando Y, Satoh K, Barada D, et al. Holographic augmented

reality display with conical holographic optical element for wide viewing zone[J]. Light: Advanced Manufacturing, 2022, 3(1): 26-34.
[5] Apai D, Milster T D, Kim D W, et al. Nautilus Observatory: a space telescope array based on very large aperture ultralight diffractive optical elements[J]. Proceedings of SPIE, 2019, 11116: 1111608.
[6] Middendorf J R, LeMaster D A, Zarepoor M, et al. Design of multi-order diffractive THz lenses[C]//2012 37th International Conference on Infrared, Millimeter, and Terahertz Waves, September 23-24, 2012, Wollongong, NSW, Australia. New York: IEEE Press, 2012.
[7] Singh M, Tervo J, Turunen J. Broadband beam shaping with harmonic diffractive optics[J]. Optics Express, 2014, 22(19): 22680-22688.
[8] Nikonorov A V, Petrov M V, Bibikov S A, et al. Toward ultralightweight remote sensing with harmonic lenses and convolutional neural networks[J]. IEEE Journal of Selected Topics in Applied Earth Observations and Remote Sensing, 2018, 11(9): 3338-3348.
[9] 巩畅畅, 刘鑫, 范斌, 等. 基于RGB三波段的消色差衍射透镜设计与分析[J]. 光学学报, 2021, 41(11): 1105001.
Gong C C, Liu X, Fan B, et al. Design and analysis of diffractive achromats based on RGB three-band[J]. Acta Optica Sinica, 2021, 41(11): 1105001.
[10] 赵玺竣, 范斌, 何一苇, 等. 基于可见光波段的编码优化消色差衍射透镜设计分析[J]. 光学学报, 2022, 42(13): 1305001.
Zhao X J, Fan B, He Y W, et al. Design and analysis of coding optimized achromatic diffraction lens based on visible band[J]. Acta Optica Sinica, 2022, 42(13): 1305001.
[11] 何书宸, 魏志伟, 葛睿, 等. 基于消色差超构光栅的AR显示光波导[J]. 激光与光电子学进展, 2022, 59(20): 2011016.
He S C, Wei Z W, Ge R, et al. Augmented reality display optical waveguide based on achromatic metagrating[J]. Laser & Optoelectronics Progress, 2022, 59(20): 2011016.
[12] Piao M X, Cui Q F, Zhu H, et al. Diffraction efficiency change of multilayer diffractive optics with environmental temperature [J]. Journal of Optics, 2014, 16(3): 035707.
[13] Piao M X, Cui Q F, Zhao C Z, et al. Substrate material selection method for multilayer diffractive optics in a wide environmental temperature range[J]. Applied Optics, 2017, 56 (10): 2826-2833.
[14] Sweeney D W, Sommargren G E. Harmonic diffractive lenses [J]. Applied Optics, 1995, 34(14): 2469-2475.
[15] Rossi M, Kunz R E, Herzig H P. Refractive and diffractive properties of planar micro-optical elements[J]. Applied Optics, 1995, 34(26): 5996-6007.
[16] Milster T D, Kim Y S, Wang Z C, et al. Multiple-order diffractive engineered surface lenses[J]. Applied Optics, 2020, 59(26): 7900-7906.
[17] Apai D, Milster T D, Kim D W, et al. A thousand earths: a very large aperture, ultralight space telescope array for atmospheric biosignature surveys[J]. The Astronomical Journal, 2019, 158(2): 83.
[18] Sweatt W C. Describing holographic optical elements as lenses [J]. Journal of the Optical Society of America, 1977, 67(6): 803-808.
[19] Sweatt W C. Mathematical equivalence between a holographic optical element and an ultra-high index lens[J]. Journal of the Optical Society of America, 1979, 69(3): 486-487.
[20] Kleinhans W A. Aberrations of curved zone plates and Fresnel lenses[J]. Applied Optics, 1977, 16(6): 1701-1704.
[21] Welford W T. Aberrations of optical systems[M]//Pike E R, Saleh B E A, Welford W T. The Adam Hilger series on optics and optoelectronics. England: IOP, 1986: 226-234.
[22] Buralli D A, Morris G M. Design of a wide field diffractive landscape lens[J]. Applied Optics, 1989, 28(18): 3950-3959.

Surface Analysis of Achromatic System with Multiple-Order Diffractive Element

Zheng Boyang[1,2], Xue Changxi[1,2*]

[1]*School of Optoelectronic Engineering, Changchun University of Science and Technology, Changchun* 130022, *Jilin, China*;

[2]*Key Laboratory of Advanced Optical System Design and Manufacturing Technology of Universities of Jilin Province, Changchun University of Science and Technology, Changchun* 130022, *Jilin, China*

Abstract

Objective As science and technology develop by leaps and bounds, requirements for the comprehensive performance of optical systems are getting higher. Optical systems are developing towards lightweight, simple structure, excellent optical performance, and low manufacturing cost. Due to its good optical properties, thermal stability, and flat field characteristics, the diffractive optical element is applied to the achromatic field. It can not only increase the degree of freedom of optical design but also break through many limitations of traditional optical systems. It has incomparable advantages in improving the image quality and reducing the volume and weight of the system, whereas its dispersion characteristics limit the application in the wide band. In this paper, a combination of multiple-order diffractive elements (MODs), refractive elements (ROEs), and diffractive Fresnel elements (DFLs) is proposed to realize the achromatism of the system, which greatly enhances the practicability of diffractive lenses under the wide band. In the field of wide band, the achromatic and apochromatic refractive-diffractive hybrid optical system can be realized. After analyzing and comparing surface shapes, the results which can optimize the imaging quality of the optical system are obtained. The proposed design

can promote the application of the refractive-diffractive hybrid optical system in the field of achromatic and be conducive to the application of multiple-order diffractive element combination system in the field of achromatic.

Methods This paper analyzes the optical system composed of multiple-order diffractive elements, refractive elements, and diffractive Fresnel elements. Under the guidance of scalar diffraction theory, the combined optical system is mathematically expressed based on the Seidel third-order aberration theory. Firstly, according to the achromatic and apochromatic characteristics of the system, the focal power of the system is expressed, and the expression relationship is obtained. Then, according to the third-order aberration theory of the thin lens, the third-order aberration coefficients of the three elements after gluing are obtained, and the conjugate parameters and bending parameters of the system are expressed by the definition and relational expression of the conjugate angle of the thin lens. By the given specific parameters, an achromatic and apochromatic system based on the proposed design concept is obtained, and the spherical aberration and coma aberration of the system are corrected. A better surface is selected after the three optical elements and comparing their different surface morphologies are analyzed. The achromatic and imaging quality of the three elements are compared mainly from the three modes of planar, spherical, and aspheric surfaces.

Results and Discussions Through the mathematical derivation of the system, the Seidel aberration coefficients of the spherical aberration and coma of the system are set to zero respectively. Via the given parameters, a three-element glued optical system with corrected spherical aberration and achromatic and apochromatic aberration is obtained (Fig. 3). Then, the system is placed under the base surface of planar, spherical, and aspheric surface respectively, and some of its parameters are controlled to be the same (Table 1). By changing its aspheric coefficient and radian coefficient (Table 2), a comparative analysis is carried out under the optical system with a focal length f=20 mm, a field of view of 3.5°, an F number of 4, and a working band of 400-700 nm in the visible light band. It is concluded that the system has a better quality under spherical and aspheric surfaces (Fig. 5), smaller axial aberration, and a more obvious achromatic effect (Fig. 6), which is markedly better than under the plane surface. The modulation transfer function and the encircled energy of the spherical and aspheric surfaces are compared. It is concluded that when the system is an aspheric surface, the modulation transfer function of the system is 0.6683, which is much higher than that of the system with the spherical surface (0.3653), and the encircled energy is also higher (Fig. 7). Therefore, the three-element combined system is more suitable for achromatic requirements and has a better imaging quality when the aspheric surface is used.

Conclusions In this paper, the optical system composed of MOD, ROE, and DFL is analyzed based on the third-order aberration theory of Seidel. In the given working band of 400-700 nm, the expression and calculation of the system bending parameters, conjugate parameters, and lens curvature are utilized to simultaneously correct the spherical aberration and coma aberration of the three-element glued refractive-diffractive hybrid achromatic system. The surface shape of the system is analyzed, and the achromatic situation and the imaging quality of the system with the planar, spherical, and aspheric surfaces are compared. It is found that the imaging quality of the system is better, the diffraction energy is more, and the achromatic effect is more obvious when the system is aspherical. The imaging optical system with spherical, aspheric, or free-form surface has a higher design freedom and a stronger aberration correction ability than that with the traditional planar surface. It also undertakes more tasks of balancing aberrations in the system and is easier to achieve the design goal of miniaturization and lightweight of the system. The designed system designed has small size, lightweight, and simple structure, which has broad application prospects in the field of space optics.

Key words diffraction; multiple-order diffraction element; third-order aberration theory; achromatism; aspheric surface; hybrid refraction/diffraction